Research Square

Preprints are preliminary reports that have not undergone peer review.
They should not be considered conclusive, used to inform clinical practice,
or referenced by the media as validated information.

Influence of spatial connectivity on the spread of Mpox in Maï-Ndombe province, Democratic Republic of the Congo, 2025

Christian Ibolobolo

christianibolobolomobali@gmail.com

University of Kinshasa

Harry Kayembe

University of Kinshasa

Didier Bompangue

Chrono-Environment Laboratory

Dav Ebengo

University of Kinshasa

Research Article

Keywords: Human mobility, Infectious disease transmission, Maï-Ndombe Province, Mpox, Spatial connectivity

Posted Date: February 10th, 2026

DOI: https://doi.org/10.21203/rs.3.rs-8711349/v1

License: This work is licensed under a Creative Commons Attribution 4.0 International License.
Read Full License

Additional Declarations: No competing interests reported.

Version of Record: A version of this preprint was published at International Journal of Health Geographics on August 17th, 2026. See the published version at https://doi.org/10.1186/s12942-026-00487-1.

1. **Title**

Influence of spatial connectivity on the spread of Mpox in Maï-Ndombe province, Democratic Republic of the Congo, 2025

Authors

1. Christian Mobali Ibolobolo[1], Harry Kayembe[1], Didier Bompangue[1,3], Dav Ebengo[1,2]
2. **corresponding author**

Christian Mobali Ibolobolo : christianibolobolomobali@gmail.com

Affiliations

1. Institut One Health pour l'Afrique (INOHA), University of Kinshasa, Kinshasa, Democratic Republic of the Congo
2. Institut National de Recherche Biomédical (INRB), Kinshasa, Democratic Republic of the Congo
3. Chrono-Environnement, UMR CNRS 6249, Université de Franche-Comté, Besançon, France

Abstract

Background: The spread of Mpox in the DRC is strongly influenced by human mobility in a context of environmental constraints and inequalities in accessibility. The province of Maï-Ndombe, with its fragmented transport network and dependence on waterways, is a relevant setting for analyzing the impact of spatial connectivity on epidemic dynamics.

Objective: Quantify spatial connectivity in the area and assess its influence on the spread of Mpox in Maï-Ndombe province

Methods: A spatial connectivity analysis based on a gravity model integrating demographic attractiveness and distance-cost (slope, land use) was combined with a spatialized SEIR model.

Inter-zone flows, centrality, and accessibility were quantified. The performance of SEIR models with and without connectivity was compared using RMSE, MAE, and precision gain per zone.

Results: Flows are concentrated around pivotal areas (Bokoro, Nioki, Mushie), while peripheral areas remain isolated, with accessibility mainly provided by river corridors. The integration of connectivity degrades the overall fit of the model, but improves forecasts in highly connected areas and deteriorates them in poorly connected areas, reflecting marked spatial heterogeneity.

Conclusion: Connectivity does not strengthen the overall prediction of incidence, but structures the spatial redistribution of risk. These results highlight the importance of targeting interventions in areas with high connectivity, while considering the limitations of local surveillance systems.

3. Mots-clés

Human mobility

Infectious disease transmission

Maï-Ndombe Province

Mpox

Spatial connectivity

4. Background

Human mobility is a key determinant in the spread of infectious diseases, as it shapes the frequency, spatial extent, and temporal dynamics of pathogen transmission (1). Daily commutes, seasonal migrations, and economic exchanges reconfigure contact networks and promote the emergence of epidemic outbreaks in previously unexposed areas, particularly when surveillance systems remain limited. Empirical data show that the structure of mobility flows determines the spatial and temporal spread of epidemics (2,3). During the COVID-19 pandemic, interurban

connectivity determined the initial rate of spread (4). For dengue, chikungunya, and Zika, human mobility was a greater factor in the persistence of outbreaks than climatic factors (5). Similarly, during the Ebola epidemics, reduced travel slowed transmission, while revealing the critical role of secondary roads in local spread (6).

In Africa, the resurgence of Mpox reveals a spread dynamic largely influenced by intra- and inter-regional human mobility and spatial connectivity between rural and urban areas (7).

Mpox was first identified in humans in the Democratic Republic of Congo in 1970. It is a viral zoonosis comprising two distinct clades, each subdivided into two subclades. Subclade IIb was responsible for the 2022 global epidemic, characterized mainly by sexual transmission, leading to the declaration of the first public health emergency of international concern by the World Health Organization (8). Between 2022 and 2025, Mpox spread to 127 non-endemic countries and generated more than 158,425 cases worldwide. In the DRC, massive internal displacement, cross-border flows, and rapid urbanization contributed to the geographical spread of the disease and marked heterogeneity in its spatial incidence (7).

Population movements between the DRC and its neighboring countries (Uganda, Rwanda, Burundi) play an important role in the cross-border spread of Mpox (9). In 2025, more than 1.6 million people were displaced within the DRC, bringing the total number of internally displaced persons to approximately 5.28 million (10). In the same year, cases were reported in Kongo Central and several outbreaks were observed in Kinshasa, closely associated with human mobility (8). In South Kivu, an outbreak that appeared in Kamituga in 2024 affected 19 of the 34 health zones (56%) (11). Interprovincial flows, particularly between Kwilu, Kwango, Maï-Ndombe, and Kinshasa (196,772 displacements compared to 167,499 returns), are accompanied by an expansion into previously non-endemic rural areas, such as Bokoro, in a province where waterways structure spatial connectivity (12).

The province of Maï-Ndombe is a particularly good example of the above-mentioned dynamics. Predominantly rural and characterized by a high degree of ecosystem diversity, it relies mainly on waterways as its primary networks for travel and trade (13). Environmental constraints, such as dense forests, seasonal floodplains, and limited road accessibility, create stark contrasts in spatial connectivity between health zones (13). In this context, cases of Mpox show a heterogeneous spatial distribution, suggesting that transportation networks and physical barriers play a structuring role in the spread of the disease.

The analysis of the spatial dynamics of infectious diseases is based on a set of approaches that explicitly integrate human mobility. Bayesian geostatistical models, sometimes coupled with stochastic partial differential equations, have been used to describe the spatiotemporal structures of epidemics such as Ebola (14). Deterministic compartmental models, particularly SEIR models, have been used to analyze the spread of COVID-19 and the importation of cases (15), while metapopulational models have highlighted the role of mobility in the persistence of malaria. Stochastic approaches incorporating mobility data have been applied to Zika, and generalized linear models have examined the association between transport flows and Mpox incidence (5,14,15). In parallel, accessibility and spatial connectivity are traditionally assessed using gravity models, 2SFCA methods, network analysis, distance-cost algorithms, and circuit theory (16,17).

In remote rural areas such as Maï-Ndombe province, human mobility is a factor in the spread of emerging pathogens, although its structural mechanisms remain poorly understood(18). In this context, dominated by river networks and a limited road network, the spatial spread of Mpox remains poorly understood due to the scarcity of mobility data and the fragility of surveillance systems, which limits the performance of epidemiological models and the relevance of targeted interventions (19,20).

In the absence of empirical data, gravity models offer a functional approximation of spatial connectivity (21). The integration of environmental and topographical constraints and river and road networks improves the estimation of travel costs in areas with poor accessibility, but their structural simplicity limits the consideration of the heterogeneity and variability of transmission dynamics (21–23). In a contrasting epidemiological context, marked in 2022 by the coexistence of the Mpox clade Ib in the DRC, detailed characterization of local spread mechanisms appears essential. The challenge now is to strengthen these approaches in order to produce more robust and operational modeling tools for anticipating epidemic risk in tropical forest environments.

In this context, this study aims to quantify the spatial connectivity between health zones in Maï-Ndombe using an enhanced gravity model, then to assess its influence on the spread of Mpox between 2022 and 2025 by coupling it with a spatialized SEIR model, in order to assess the epidemiological added value of explicitly integrating inter-zone mobility.

Methods

Study area

The province of Maï-Ndombe is located in the central basin. From east to west and north to south, the terrain is low and monotonous, with an average altitude of 500 m.

The province of Maï-Ndombe has a variety of land uses dominated by tropical rainforest, which covers approximately 11,403.8 km², or 87% of the area, including the territories of Oshwe, Kiri, Inongo, and northern Kutu. Apart from the majority of vegetation cover consisting of dense rainforests, 15.93% of the forests are on hydromorphic soils. In contrast, the south and southwest of the province, particularly the territories of Bolobo, Mushie, Kwamouth, Yumbi, and southern Kutu, are characterized by a savanna landscape punctuated by fragments of forest and forest galleries (13). The geographical location of the province and its health subdivisions are presented in Figure 1.

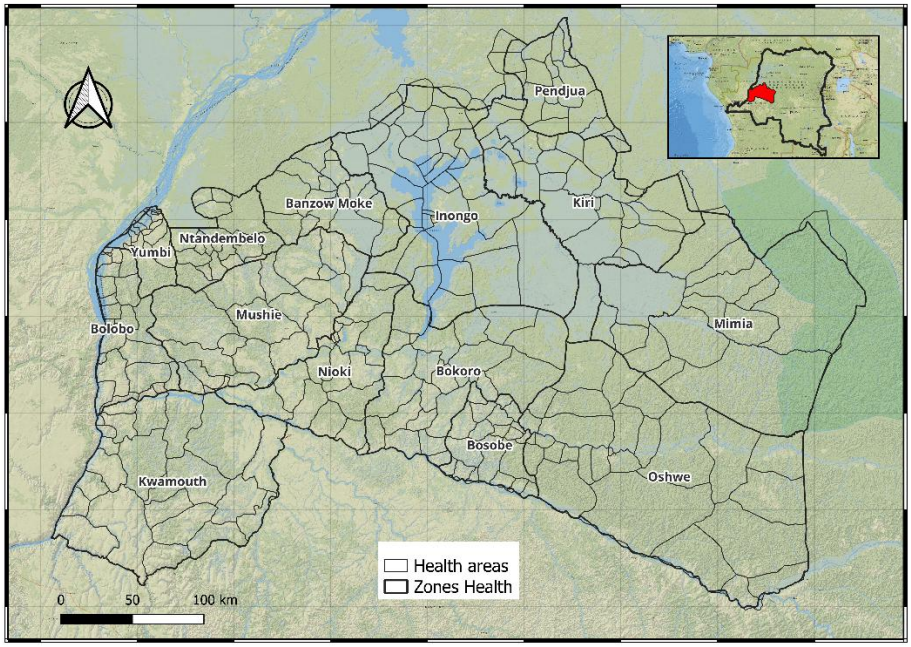


Figure 1. Geographical location of the province of Maï-Ndombe in the Democratic Republic of Congo, showing the health zones.

Data sources and collection

Land cover

MODIS Land Cover (MCD12Q1, version 6.1) land cover data was downloaded from https://search.earthdata.nasa.gov/search. The 2022 images were obtained with a spatial resolution of 500 m. These data were used after reclassification into five classes: forest, forest mosaic, hydromorphic areas, savanna, and water bodies.

Topography

SRTM 30m data was downloaded from https://earthexplorer.usgs.gov/ to produce an elevation map of the study area at a resolution of 30m. The DTM was pre-processed to correct for gaps, and the resulting data highlights the topographical variations of the territory.

Transports

Data on transport routes, roads, and rivers in the study area were downloaded from https://data.humdata.org/

To obtain a reliable and usable network, this data was cleaned up: duplicates were removed, invalid geometries were corrected, section continuity was verified, and attributes (road type, navigability of waterways) were harmonized.

Population

The population data used for the study comes from https://human-settlement.emergency.copernicus.eu/ghs_pop.php. This product provides estimates of population density and distribution at a fine scale of 250 m pixels for the entire study area (24). The population used in this study does not take into account births and deaths but uses all simulated populations up to 2030. The original population was set by national regulations: areas with fewer than 50,000 inhabitants are considered to be of origin, and those with more than 50,000 inhabitants are considered to be of destination.

Epidemiological data

Data on Mpox cases were downloaded from the database https://dhis2.org/fr/downloads/. They were adjusted before being used. This process was based on the surveillance adequacy score (SAS) to correct for systematic underreporting bias (19). Stochastic modeling using Monte Carlo simulation was used to quantify uncertainties related to geographical isolation, seasonal diagnostic confusion, the population's perception of the disease, diagnosis including positive predictive value, and case reporting.

Modeling

Model calibration

Given the lack of data on human mobility flows, the calibration of barrier effects (slope and each component of land cover) was performed using the Fuzzy-AHP method (25). This approach

allows the coefficients to be weighted taking into account the uncertainty of subjective judgments through the use of triangular fuzzy numbers. The steps are as follows:

Fuzzification

To quantify the relative importance of the criteria, Saaty's scale (25), adapted to fuzzy logic, was used. The criteria selected were: Forest (FR), Water (Wa), Forest Mosaic (FM), Hydromorphic Zones (HZ), Savannah (SA) and Slope (Sl). A comparison matrix between the criteria was created and the qualitative judgments were converted into Triangular Fuzzy Numbers (TFN). Comparing citerions i with citerions j, we obtains :

$$\boldsymbol{a_{ij} = (I_{ij}, m_{ij,} u_{ij})}$$

Where Iij, mij, and uij represent the minimum, most probable, and maximum values, respectively, of the importance rating of criterion iii relative to criterion jjj.

Calculation of synthetic ranges (Si)

For criterion i among n criteria, the synthetic fuzzy weight is calculated in two steps:

Sum of the rows of the matrix**:**

$$\sum_{j=1}^{n} \tilde{\boldsymbol{a}}_{ij} = (\sum_{j=1}^{n} \boldsymbol{l}_{ij}, \sum_{j=1}^{n} \boldsymbol{m}_{ij}, \sum_{j=1}^{n} \boldsymbol{u}_{ij})$$

The synthetic value

$$\boldsymbol{S_i} = \sum_{i=1}^{n} \tilde{\boldsymbol{a}}_{ij} \otimes \left[\sum_{i=1}^{n}\sum_{i=1}^{n} \tilde{\boldsymbol{a}}_{ij}\right] - \mathbf{1}$$

Defuzzification (Chang's method)

Each $\tilde{s}_i$ is compared to the other $\tilde{s}_k$. The degree of possibility that $\tilde{s}_1 \geq \tilde{s}_2$ is :

175 $$V(S_1 \geq S_2) = \begin{cases} 1 & si\ m_1 \geq m_2 \\ 0 & si\ l_2 \geq u_1 \\ \dfrac{l_2 - u_1}{(m_1 - u_1) - (m_2 - l_2)} & Sinon \end{cases}$$

176 Then, the non-normalized weight w'_i is the minimum of the probabilities

177 $$W'_i = \min V\,(S_i \geq S_k)\ pour\ k = 1, \ldots . n, k \neq 1$$

178 **Normalization**

179 To obtain final weights whose sum equals 1, each defuzzified weight is divided by the total sum
180 of the weights:

181 $$W_i = \frac{W'_i}{\sum_{i=1}^{n} W'_i}$$

182 To calculate the basic friction, given a specific land use i : $f_i = W_i \frac{1}{V_i}$ où W_i where Wi is the

183 normalized weight of the criterion and Vi is the permitted speed on this segment. The inverse of

184 the speed $1/V_i$ is used because the higher the speed, the lower the friction.

185

186 With two modes of transport, friction was calculated separately for each mode. For road

187 transport, friction depended on speed (30 to 50 km/h). The Cost Value (C_{roads}) equation

188 incorporates the proportion of occupancy crossed: $C_{roads} = \sum(p_i x\ f_)_i$). The results show that

189 the weights of the occupations are: FR and E 0.31, or 31% each. HZ 0.15, or 15%, Sl: 0.12, or

190 12%, FM follows with 0.091, or 9.1%, and Sa: 0.053, or 5.3%.

191

192 Due to the lack of data on river marking zones, speed is the only friction factor taken into

193 account (5 to 10 km/h), and the cost is inversely proportional to the speed of

194 navigation : $C_{flu}\ {}^{1}/_{V_{flu}}$

Distance-Cost Connectivity Matrix

The accumulated cost equation Cacc for moving from zone A to zone B, the cost of passage (C_{ij}) is : $\boldsymbol{C_{ij} = \frac{f_1+f_2}{2} d}$ where f_1, f_2 the friction values of the two adjacent zones and d is the geographical distance between the centers of the zones.

The connectivity matrix was calculated by applying the Least-Cost Path algorithm. For each pair of zones.

Modele

The gravity model is a theoretical framework for analyzing spatial connectivity between areas. It estimates the intensity of interactions between geographical entities based on Newton's law of gravity (16). The connectivity between two areas i and j is proportional to the product of their populations and inversely proportional to the square of the distance between them.

$$\boldsymbol{F_{ij} = G.\frac{p_i.p_j}{d^2}}$$

Constraints related to topography and vegetation cover increase the effective distance between two health areas and alter the intensity and direction of flows (26). The gravity model has been enhanced to incorporate these effective distances on road and river networks, weighted by exponents and combined with friction to quantify spatial connectivity.

$$\mathbf{F_{ij}= G.\frac{p_i^{\alpha} p_j^{\beta}}{C_{ij}^{\gamma}}. exp^{(-\theta.C_{ij})}}$$

D'où :

F_{ij} Spatial connectivity flows

G : Gravity

p_i, p_j : Population of the origin and destination ZS

$\mathbf{C_{ij}}$: Distance cost derived from your connectivity matrix

γ : Friction coefficient linked to distance cost

$\text{Exp}(-\Theta.\mathbf{C_{ij}})$: Deterrence function

Validation

The structure of connectivity flows was analyzed using three approaches, combining the Gini index, the coefficient of variation, and Shannon entropy (27), in order to accurately measure inequality, dispersion, and the degree of organization of the network.

To validate the influence of spatial connectivity on the spread of Mpox in Maï-Ndombe province, the connectivity matrix was integrated into a compartmentalized SEIR (Susceptible, Exposed, Infected, and Recovered) model. The F_{ij} variable is the connectivity flow from the gravity model, acting as the inter-zone transmission vector (15).

In this metapopulational approach, the infection force is divided into two components: endogenous transmission and exogenous transmission. The system of differential equations is defined as follows :

$$\begin{cases} \dfrac{dS_i}{dt} - \beta S_i \left[\dfrac{I_i}{N_i} + \sum_{j=1, j\neq i}^{n} F_{ij} \dfrac{I_i}{N_i} \right] \\ \dfrac{dE_i}{dt} \beta S_i \left[\dfrac{I_i}{N_i} + \sum_{j=1, j\neq i}^{n} F_{ij} \dfrac{I_i}{N_i} \right] - \sigma E_i \\ \dfrac{dI_i}{dt} \sigma E_i - \gamma I_i \\ \dfrac{dR_i}{dt} \gamma I_i \end{cases}$$

D’où :

Si , Ei, Ii ,Ri Total population of zone i

β	Transmission rate
$\sigma = 1 / T_{inc}$	Progression rate (inverse of incubation time)
$\gamma = 1 / T_{inf}$	Recovery rate (inverse of infectious time)
W_{ij}	Connectivity weight between zones i and j
$\Sigma W_{ij}\ I_j/N_j$	Force d'infection reçue par la zone i depuis toutes les autres zones connectées

These variables represented the internal dynamics of each health zone; Si is the entire population of the province, E_i is the number of people likely to come into contact with a pathogen but who are asymptomatic. Ii is the number of people who are actively contagious and who travel via the transport network, and finally R_i is the number of people who have recovered or are immune (15).

In this model, local transmission ($\frac{\boldsymbol{I_i}}{\boldsymbol{N_i}}$) reflects contacts within the same health zone, while connectivity transmission $\sum \boldsymbol{F_{ij}} \frac{\boldsymbol{I_j}}{\boldsymbol{N_j}}$ captures the influence of inter-zone connectivity flows.

The model parameters were defined based on scientific literature and adjusted using sensitivity analysis. The transmission rate (β) was initially set at 0.4695 (28) and then divided between local transmission and transmission via spatial connectivity to account for inter-health zone connectivity flows according to a weighting coefficient p, reflecting the predominance of close contacts in rural areas. A sensitivity analysis was conducted for $p \in [0.6; 0.8]$ (29).

The rate of progression from the exposed state to the infectious state was defined as $\sigma = 0.8703$ per week, corresponding to an average incubation period of approximately 9 to 10 days (29). The recovery rate was set at $\gamma = 0.8023$ per week. These values fall within an observed incubation period ranging from 1 to 21 days (28).

The model's performance was evaluated using a comparative analysis of the root mean square error. The $RMSE_0$ was calculated for the SEIR model without connectivity, then the

RMSEconnect was calculated using the connectivity matrix. The specific contribution of the spatial dimension is quantified by the index $\Delta RMSE = RMSE_0 - RMSE_{connect}/RMSE_0$. This ratio measures the relative gain in accuracy: a positive value close to 1 confirms that connectivity reduces the uncertainty of predictions and allows the contribution of connectivity to the dynamics of Mpox propagation to be isolated from homogeneous diffusion.

Geographic processing, distance matrix calculations, and integration of environmental variables (DTM, land cover) were performed using Rstudio software, and visualization was performed using QGIS 3.28. For the simulation of Mpox propagation, Python was used within the Anaconda environment via the Jupyter Notebook interface.

Below, we present a synthetic view of the modeling framework, from the initial input data to the spatialized SEIR (Figure 2).

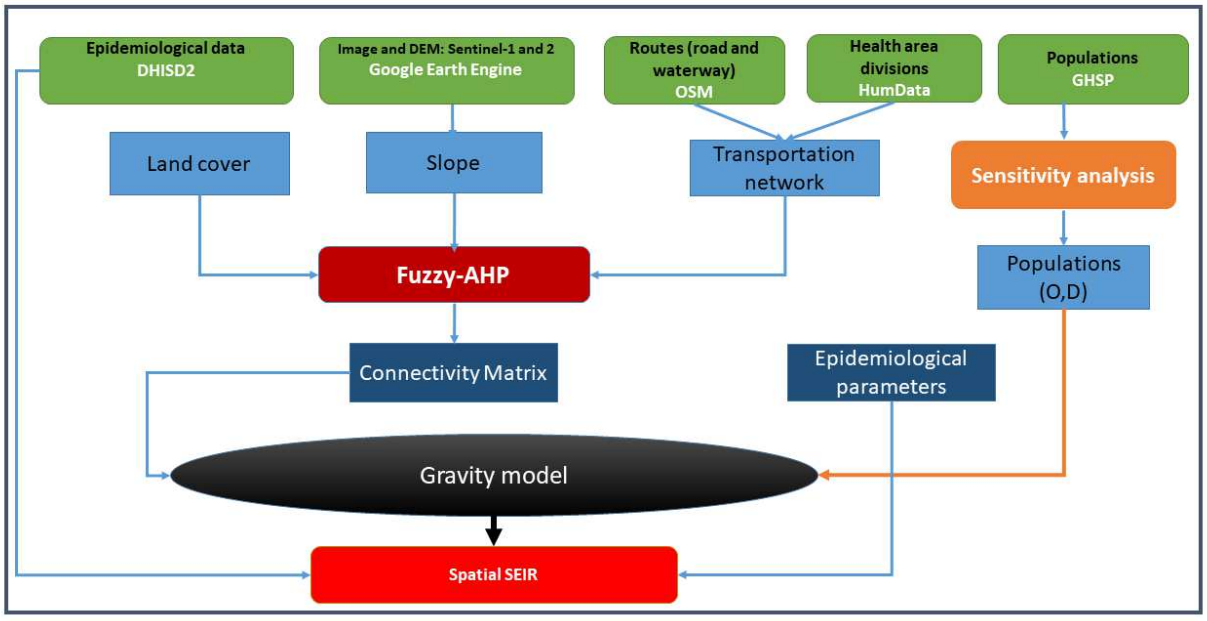


Figure 2. The summary of the overall modeling framework, illustrating the successive steps from data integration and spatial connectivity modeling to the explicit spatialized SEIR model

Results

1. Quantification of spatial connectivity in the province of Maï-Ndombe from 2022 to 2025

The connectivity flow between health zones in the province of Maï-Ndombe is calculated using a gravity model that incorporates demographic attractiveness and distance-cost, taking into account slope and land use (Figure 3). The results highlight a high concentration of flows on a limited number of axes (Gini = 0.65) (Figure 4) with marked heterogeneity (CV = 1.52) and with a flow that is not randomly dispersed throughout the province, but rather with certain axes acting as hubs (Shannon entropy 4.426423).

Gravitational centrality analysis makes it possible to determine the most connected areas of the province, and the results highlight a functional hierarchy within the connectivity network of Maï-Ndombe province (Figure 5). The areas of Bokoro (0.00147) and Mushie (0.00121) occupy strategic relay positions within the network, giving them a major role in structuring connectivity at the provincial level compared to Inongo (0.000843), Bolobo (0.000744), and Yumbi (0.00085).

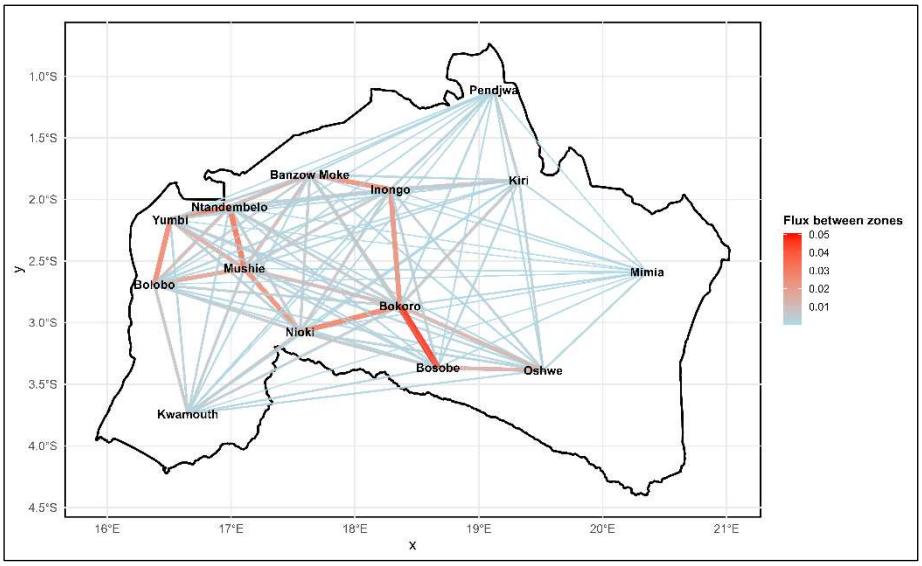


Figure 3. Spatial distribution of weighted connectivity flows between health zones in the province of Maï-Ndombe, derived from the gravity-based connectivity model.

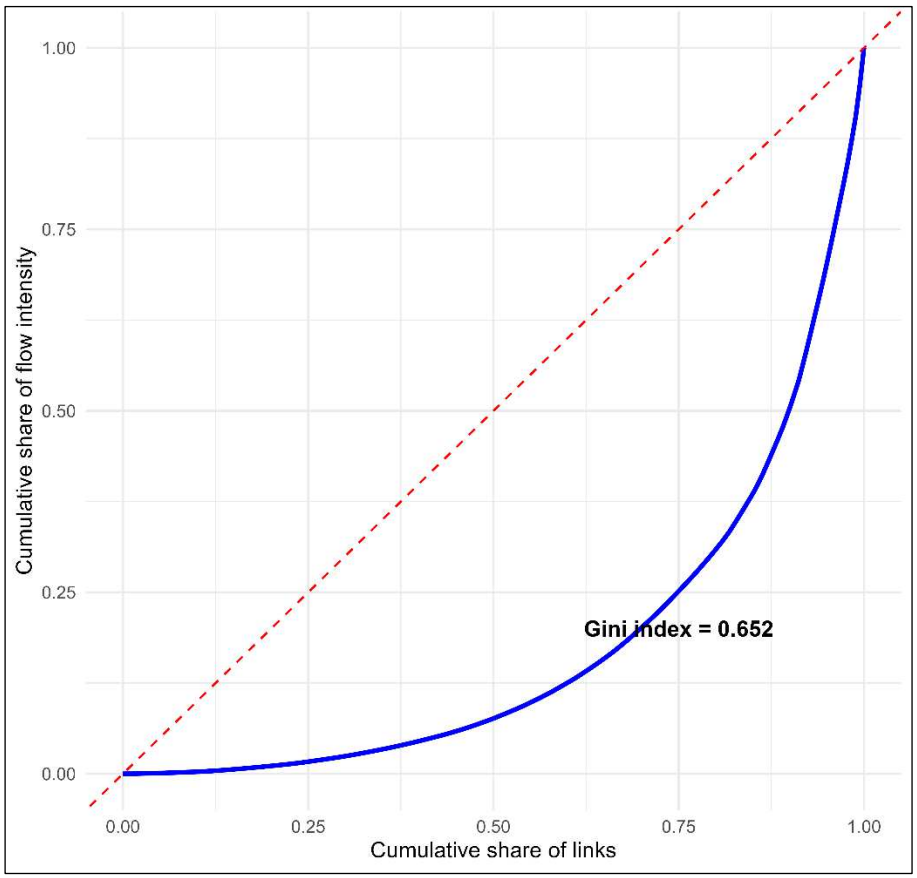


Figure 4. Lorenz curve illustrating the concentration of spatial connectivity flows between health zones in Maï-Ndombe Province, highlighting the degree of inequality in the connectivity network.

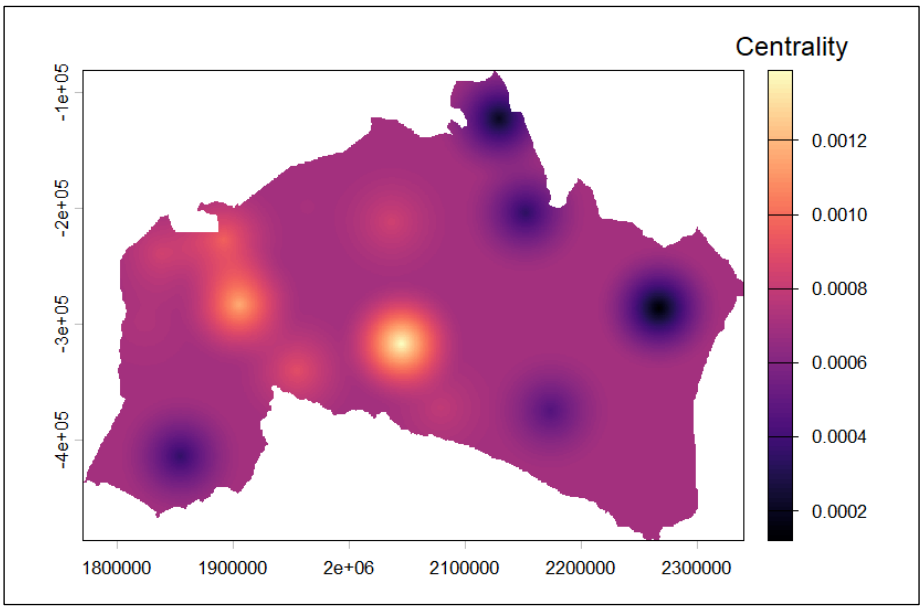


Figure 5. Spatial distribution of closeness centrality across health zones in the multimodal transport network of Maï-Ndombe Province.

Influence of spatial connectivity on the spread of Mpox in Maï-Ndombe Province

The integration of interzone connectivity flows into the spatialized SEIR model leads to a deterioration in the overall fit (ΔRMSE = −0.468), suggesting that the epidemic dynamics observed at the provincial level are mainly governed by local transmission processes. The model with connectivity has an RMSE of 44.38 and an MAE of 30.12 (Figure 6), reflecting an average discrepancy of 30 to 50 weekly cases, while the model without connectivity shows better overall performance (RMSE = 30.26; MAE = 19.44).

However, this loss of aggregate performance masks spatial heterogeneity. The precision gain analysis reveals that the integration of connectivity significantly improves the fit in areas with high connectivity, particularly Bokoro, Nioki, and Mushie, while it degrades performance in areas with low connectivity such as Penjua, Kiri, and Mimia (Figure 7).

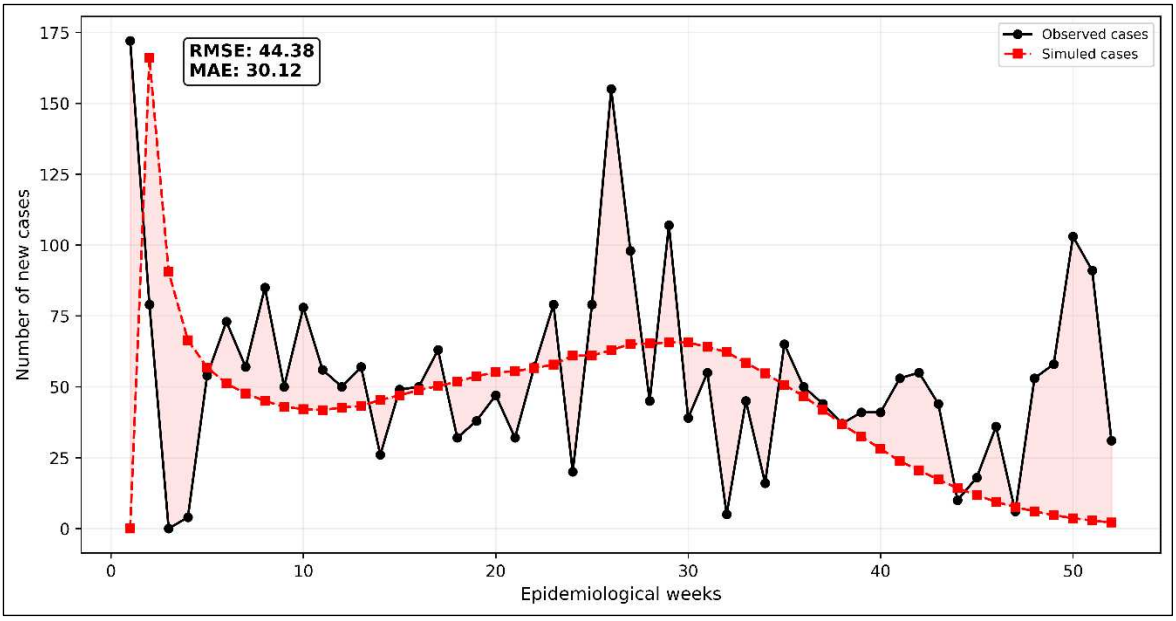


Figure 6. Comparison at provincial level of observed Mpox cases and cases simulated by the spatialized SEIR model in the province of Maï-Ndombe in 2022.

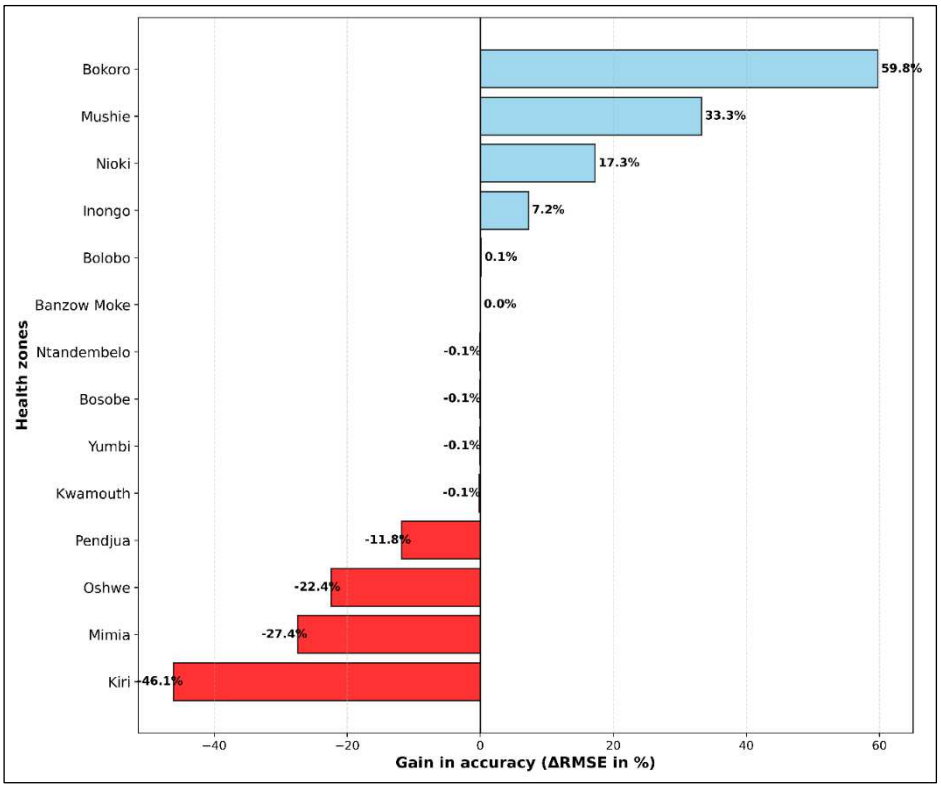


Figure 7. Changes in model performance across health zones following the integration of spatial connectivity into the SEIR model in Maï-Ndombe Province.

Discussion

Analysis of connectivity flows between health zones in Maï-Ndombe, based on a gravity model incorporating demographic attractiveness and a distance-cost factor that takes into account slope and land use, reveals a high concentration of flows on a limited number of key routes. This spatial organization is characterized by marked inequality of flows (Gini = 0.65), high heterogeneity (CV = 1.52), and moderate Shannon entropy (4.43), indicating the existence of privileged corridors acting as hubs. The health zones of Bokoro, Nioki, and Inongo have the highest flow intensities.

Bokoro appears to be a strategic crossroads connecting forest areas to evacuation points, Nioki an industrial hub with the busiest airport, and Inongo an administrative center, despite its isolation on the lake. Conversely, peripheral areas such as Mimia, Oshwe, and Kiri are structurally isolated, with low population density and high resistance to travel. In Mimia, the average distance between homes and health centers is 95 km, while Kiri is characterized by a severely degraded road network (13).

To assess the influence of this connectivity heterogeneity on Mpox spread, we use a spatial SEIR model incorporating inter-zone interactions modulated by travel costs.

The integration of spatial connectivity degrades the overall fit of the SEIR model (ΔRMSE = −0.468), confirming the predominance of local transmission at the provincial level. However, it improves the fit in highly connected areas (Bokoro, Nioki, Mushie) and degrades it in poorly connected areas (Penjua, Kiri, Mimia), revealing marked spatial heterogeneity in the effect of mobility (39,40). This limitation of the model can be explained by the nature of syndromic surveillance data, which is characterized by delays and losses in case reporting. One-off social events (markets, funerals, nganda) generate rapid transmission that is insufficiently captured,

especially during outbreaks, but also by the connectivity model, which only considers demographic flow as attractiveness (19).

Previous studies have shown that the introduction of connectivity structures can significantly alter the local dynamics of epidemics, sometimes to the detriment of aggregate adjustment (41). Heterogeneous spatial networks modulate local epidemic dynamics, even when overall dynamics remain unchanged (39). Similarly, incorporating interaction structure into metapopulation models influences invasion thresholds depending on the level of connectivity (40).

A study conducted in Bokoro highlights a low level of case reporting, attributable to sociodemographic, sociocultural, and organizational factors that lead to non-compliance with epidemiological surveillance standards (20). At the same time, markets, funerals, temporary shelters (nganda), and other social gatherings create opportunities for rapid transmission (19). In this context, discrepancies in cases reported in the spatial SEIR model are justified by the limitations of the reporting system, lack of training, lack of funding, lack of tools and means of transport, and poor understanding of epidemiological indicators and thresholds (20).

Despite limitations related to geographic isolation, surveillance data, actual mobility data, and the lack of local epidemiological parameters, this approach provides key elements for targeting surveillance and interventions in strategic areas.

Conclusion

The results of the influence of spatial connectivity on the spread of Mpox in Maï-Ndombe province show that the spread of the virus in the province is conditioned by the structure of spatial connectivity. The concentration of interactions along major river corridors and around functional hubs such as Bokoro, Nioki, and Inongo identifies these areas as epidemic hotspots requiring priority attention from surveillance interventions.

Operationally, these results call for targeted strengthening of epidemiological surveillance in areas with high centrality, particularly at river transport hubs and at the interfaces between forest and savanna areas. The establishment of sentinel sites in these strategic areas would enable early detection of cases and better anticipation of outbreaks, particularly in a context of persistent underreporting. The structuring of connectivity flows around waterways highlights the need to fully integrate river transport into Mpox control strategies.

Awareness-raising, community screening, and mobile surveillance activities should be deployed along major waterways such as the Congo River, the Kasai River, and the Lukenie and Mfimi rivers, particularly during periods of high seasonal mobility and large social gatherings (markets, funerals, temporary settlements).

Furthermore, the isolation of the Mimia, Oshwe, and Kiri areas, combined with high travel costs, requires the development of differentiated strategies. In these isolated areas, improving access to care, strengthening the capacities of community relays, and providing logistical support for the collection of epidemiological data are essential levers for limiting delays in detection and the silent spread of the disease.

Finally, the observed limitations of the model, linked to the lack of local estimates of R_0 and R_t and the inadequacies of the syndromic surveillance system, underscore the urgency of producing more robust local epidemiological data. The development of surveillance tools that integrate human mobility, spatial connectivity, and sociocultural dynamics appears essential to improve preparedness and response to future Mpox outbreaks in Maï-Ndombe province.

Conflict of interest

The authors declare no conflict of interest. The research was conducted in the absence of any financial, institutional, or personal relationships that could have influenced the study design, data analysis, interpretation of the results, or the writing of the manuscript.

Author Contributions

1. **Christian Ibolobolo:** Conceptualization, methodology development, spatial connectivity and epidemiological modeling analysis, data interpretation, and original draft preparation.
2. **Professor Harry Kayembe:** Critical review and editing of the manuscript.
3. **Professor Didier Bompangue:** Contribution to the discussion and scientific validation.
4. **Professor Dav Ebengo:** Project administration, general supervision, and final validation of the work.

Acknowledgments

The authors would like to express their sincere gratitude to Professor Didier Bompangue,Professor Harry Kayembe, and Professor Dav Ebengo for their scientific guidance, methodological advice, and continuous support throughout the completion of this work.

Bibliographical references

1. Brockmann D. Human Mobility, Networks and Disease Dynamics on a Global Scale. In: Bunde A, Caro J, Kärger J, Vogl G, éditeurs. Diffusive Spreading in Nature, Technology and Society [Internet]. Cham: Springer International Publishing; 2018 [cité 14 févr 2025]. p. 375-96. Disponible sur: https://doi.org/10.1007/978-3-319-67798-9_19

2. Findlater A, Bogoch II. Human Mobility and the Global Spread of Infectious Diseases: A Focus on Air Travel. Trends Parasitol. sept 2018;34(9):772-83.

3. Wesolowski A, Qureshi T, Boni MF, Sundsøy PR, Johansson MA, Rasheed SB, et al. Impact of human mobility on the emergence of dengue epidemics in Pakistan. Proc Natl Acad Sci. 22 sept 2015;112(38):11887-92.

4. Wan L, Wan Q. High-speed railway and the intercity transmission of epidemics: Evidence from COVID-19 in China. Econ Model. sept 2022;114:105934.

5. Weaver SC, Charlier C, Vasilakis N, Lecuit M. Zika, Chikungunya, and Other Emerging Vector-Borne Viral Diseases. Annu Rev Med. 29 janv 2018;69:395-408.

6. Barbieri DM, Lou B, Passavanti M, Hui C, Hoff I, Lessa DA, et al. Impact of COVID-19 pandemic on mobility in ten countries and associated perceived risk for all transport modes. PloS One. 2021;16(2):e0245886.

7. Akingbola A, Adegbesan CA, Adewole O, Idahor C, Odukoya T, Nwaeze E, et al. Understanding the resurgence of mpox: key drivers and lessons from recent outbreaks in Africa. Trop Med Health. 3 avr 2025;53:47.

8. Karagoz A, Tombuloglu H, Alsaeed M, Tombuloglu G, AlRubaish AA, Mahmoud A, et al. Monkeypox (mpox) virus: Classification, origin, transmission, genome organization, antiviral drugs, and molecular diagnosis. J Infect Public Health. 1 avr 2023;16(4):531-41.

9. Ugwu ISO Faridat Ibidun, Samuelii O Alawode, Mujib O Surakat, Vivian. Paradoxical Disparities in the 2024 MPOX Outbreak Between Two Neighboring Countries: Rwanda and Burundi. Medtigo J Med [Internet]. 7 oct 2024 [cité 12 janv 2026];2(4). Disponible sur: https://journal.medtigo.com/paradoxical-disparities-in-the-2024-mpox-outbreak-between-two-neighboring-countries-rwanda-and-burundi/

10. DTM_DRC_InternalDisplacementOverview_2024_FR_PUBLIC.

11. Masirika LM, Kumar A, Dutt M, Ostadgavahi AT, Hewins B, Nadine MB, et al. Complete Genome Sequencing, Annotation, and Mutational Profiling of the Novel Clade I Human Mpox Virus, Kamituga Strain. J Infect Dev Ctries. 30 avr 2024;18(4):600-8.

INTERNATIONAL ORGANIZATION FOR MIGRATION (IOM). *Rapid Displacement Analysis - DRC Western Region*. Kinshasa: IOM DRC, October 2025. [Accessed 16 January 2026].

13. Omasombo Tshonda, J. (dir.). (2019). *République démocratique du Congo : MAI-NDOMBE. Mosaïque de peuples établie sur un patrimoine naturel*. Tervuren : Musée royal de l'Afrique centrale (Coll. « Monographies des provinces de la République démocratique du Congo », n° 12)

14. Brockmann D. Human Mobility and Spatial Disease Dynamics. In: Schuster HG, éditeur. Reviews of Nonlinear Dynamics and Complexity [Internet]. 1re éd. Wiley; 2009 [cité 1 févr 2025]. p. 1-24. Disponible sur: https://onlinelibrary.wiley.com/doi/10.1002/9783527628001.ch1

15. Hatami F, Chen S, Paul R, Thill JC. Simulating and Forecasting the COVID-19 Spread in a U.S. Metropolitan Region with a Spatial SEIR Model. Int J Environ Res Public Health. janv 2022;19(23):15771.

16. Piovani D, Arcaute E, Uchoa G, Wilson A, Batty M. Measuring accessibility using gravity and radiation models. R Soc Open Sci. 12 sept 2018;5(9):171668.

17. Chen Y. The distance-decay function of geographical gravity model: Power law or exponential law? Chaos Solitons Fractals. 1 août 2015;77:174-89.

18. rapid-risk-assessment_-mpox_global_v.3.

19. Mandja BAM, Bompangue D, Handschumacher P, Gonzalez JP, Salem G, Muyembe JJ, et al. The score of integrated disease surveillance and response adequacy (SIA): a pragmatic score for comparing weekly reported diseases based on a systematic review. BMC Public Health. 22 mai 2019;19(1):624.

20. Fernand MT, Camile LB, Modjou M, Londjiringa EL, Guylit KL, Grace PN, et al. Statistical Analysis of Factors Associated with Non-Compliance with Epidemiological Standards in the Bokoro Health Zone (2021 To 2023). Asian J Probab Stat. 13 févr 2025;27(3):24-42.

21. Gu H, Shen ,Jianfa, and Chu J. Understanding Intercity Mobility Patterns in Rapidly Urbanizing China, 2015–2019: Evidence from Longitudinal Poisson Gravity Modeling. Ann Am Assoc Geogr. 2 janv 2023;113(1):307-30.

22. Zhao Y, Cheng S, Gao S, Lu F. A gravity-inspired model integrating geospatial and socioeconomic distances for truck origin–destination flows prediction. Int J Appl Earth Obs Geoinformation. 1 févr 2025;136:104328.

23. Barrios JM, Verstraeten WW, Maes P, Aerts JM, Farifteh J, Coppin P. Using the Gravity Model to Estimate the Spatial Spread of Vector-Borne Diseases. Int J Environ Res Public Health. déc 2012;9(12):4346-64.

24. Carioli A, Schiavina M, MacManus KJ, Freire S. GHS-POP R2023A - GHS population grid multitemporal (1975-2030). 8 mai 2023 [cité 7 janv 2026]; Disponible sur: http://data.europa.eu/89h/2ff68a52-5b5b-4a22-8f40-c41da8332cfe

25. Kumar M, Singh P, Singh P. Fuzzy AHP based GIS and remote sensing techniques for the groundwater potential zonation for Bundelkhand Craton Region, India. Geocarto Int. 16 sept 2022;37(22):6671-94.

26. Luo W, Wang F. Measures of Spatial Accessibility to Healthcare in a GIS Environment: Synthesis and a Case Study in Chicago Region. Environ Plan B Plan Des. déc 2003;30(6):865-84.

27. Tivadar M, Schaeffer Y, Torre A, Bray F. OASIS – un Outil d'Analyse de la Ségrégation et des Inégalités Spatiales. Cybergeo Eur J Geogr [Internet]. 20 déc 2014 [cité 2 janv 2026]; Disponible sur: https://journals.openedition.org/cybergeo/26579

28. Idisi IO, Oshinubi K, Sewanu VB, Yahaya MM, Olagbami OS, Edogbanya HO. Investigating Mpox Strain Dynamics Using Computational and Data-Driven Approaches. Viruses. févr 2025;17(2):154.

29. Marziano V, Guzzetta G, Longini I, Merler S. Epidemiologic Quantities for Monkeypox Virus Clade I from Historical Data with Implications for Current Outbreaks, Democratic Republic of the Congo. Emerg Infect Dis. oct 2024;30(10):2042-6.

30. The Gravity Model in Transportation Analysis: Theory and Extensions - Sven Erlander, Neil F. Stewart - Google Livres [Internet]. [cité 30 oct 2025]. Disponible sur: https://books.google.cd/books/about/The_Gravity_Model_in_Transportation_Anal.html?id=tId3PU1leR8C&redir_esc=y

31. Liu Y, Cao X, Li T. Influence of Accessibility on Land Use and Landscape Pattern Based on Mapping Knowledge Domains: Review and Implications. J Adv Transp. 2020;2020(1):7985719.

32. Nir N, Knitter D, Hardt J, Schütt B. Human movement and gully erosion: Investigating feedback mechanisms using Frequency Ratio and Least Cost Path analysis in Tigray, Ethiopia. PLOS ONE. 5 févr 2021;16(2):e0245248.

33. Peptenatu D, Andronache I, Marin M, Ahammer H, Radulovic M, Jelinek HF, et al. Using Succolarity as a Measure of Slope Accessibility in Undeveloped Areas. Land. nov 2025;14(11):2171.

34. Geza T, Kincses Á. Accessibility Models Based On the Gravity Analogy: In Theory and Practice. Reg Stat. 7 sept 2015;5:137-58.

35. Wesolowski A, O'Meara WP, Eagle N, Tatem AJ, Buckee CO. Evaluating Spatial Interaction Models for Regional Mobility in Sub-Saharan Africa. PLoS Comput Biol. 9 juill 2015;11(7):e1004267.

36. Rabino GA, Occelli S. Understanding spatial structure from network data : theoretical considerations and applications. Cybergeo Eur J Geogr [Internet]. 26 juin 1997 [cité 22 déc 2025]; Disponible sur: https://journals.openedition.org/cybergeo/2199

37. Shen L, Lv X, Zhang S, Chen P, Cheng P, Liu S. The Structural and Functional Development of an Urban Network System from the Perspective of Flow Space: A Case Study of Nanjing. Land. juill 2024;13(7):1099.

38. Rocha TAH, Silva LL, Wen FH, Sachett J, Tupetz A, Staton CA, et al. River dataset as a potential fluvial transportation network for healthcare access in the Amazon region. Sci Data. 6 avr 2023;10(1):188.

39. Thomas LJ, Huang P, Yin F, Luo XI, Almquist ZW, Hipp JR, et al. Spatial Heterogeneity Can Lead to Substantial Local Variations in COVID-19 Timing and Severity. Proc Natl Acad Sci. 29 sept 2020;117(39):24180-7.

40. Colizza V, Vespignani A. Invasion threshold in heterogeneous metapopulation networks. Phys Rev Lett. 5 oct 2007;99(14):148701.

41. Lee SA, Jarvis CI, Edmunds WJ, Economou T, Lowe R. Spatial connectivity in mosquito-borne disease models: a systematic review of methods and assumptions. J R Soc Interface. 18(178):20210096.